Chapter 3

Experimental
and
Analytical Techniques

3.1 Introduction

Plasma Enhanced Chemical Vapor Deposition (PECVD) technique is the most popular method utilized in the preparation of silicon carbide thin films. In this work, silicon carbide thin films were prepared using a locally designed reaction chamber together with an adjustable home-built deposition system. The deposition system was made to be able to produce thin films using direct current (DC-PECVD), radio frequency (RF-PECVD) and hot-wire (HW-CVD). The special feature of this home-built system is that it is capable of producing thin films through a combination of direct current and hot-wire techniques. The combination method was named as hot-wire plasma enhanced chemical vapor deposition (HW-PECVD). This chapter describes the experimental part of producing silicon carbide thin films through all the mentioned deposition techniques. Analytic methods used in the study of the prepared silicon carbide thin films will also be discussed in this chapter. The characterization procedures and the calculation techniques used to analyze results obtained from the measurements are detailed.

3.2 The Experimental Set-up

The experimental set-up of the deposition system was mainly consists of a deposition chamber, a diffusion pump, a rotary pump and a detoxification system. Figure 3.1 shows a schematic diagram of an overall view of the deposition system. The deposition chamber was the plasma reaction chamber and was specially designed from stainless steel to obtain good vacuum and to withstand corrosive gases such as silane. In this design, plasma gas discharge was produced vertically above a horizontal substrate holder. The diffusion pump and the rotary pump help to maintain desired deposition pressure besides playing an important role in the evacuation process. The detoxification

system was an indispensable part of the system that functions to dilute excess and toxic gases especially silane. Detailed operational procedures were explained later in this chapter. Figure 3.2 shows a detailed diagram of the deposition chamber that was connected directly to the diffusion pump.

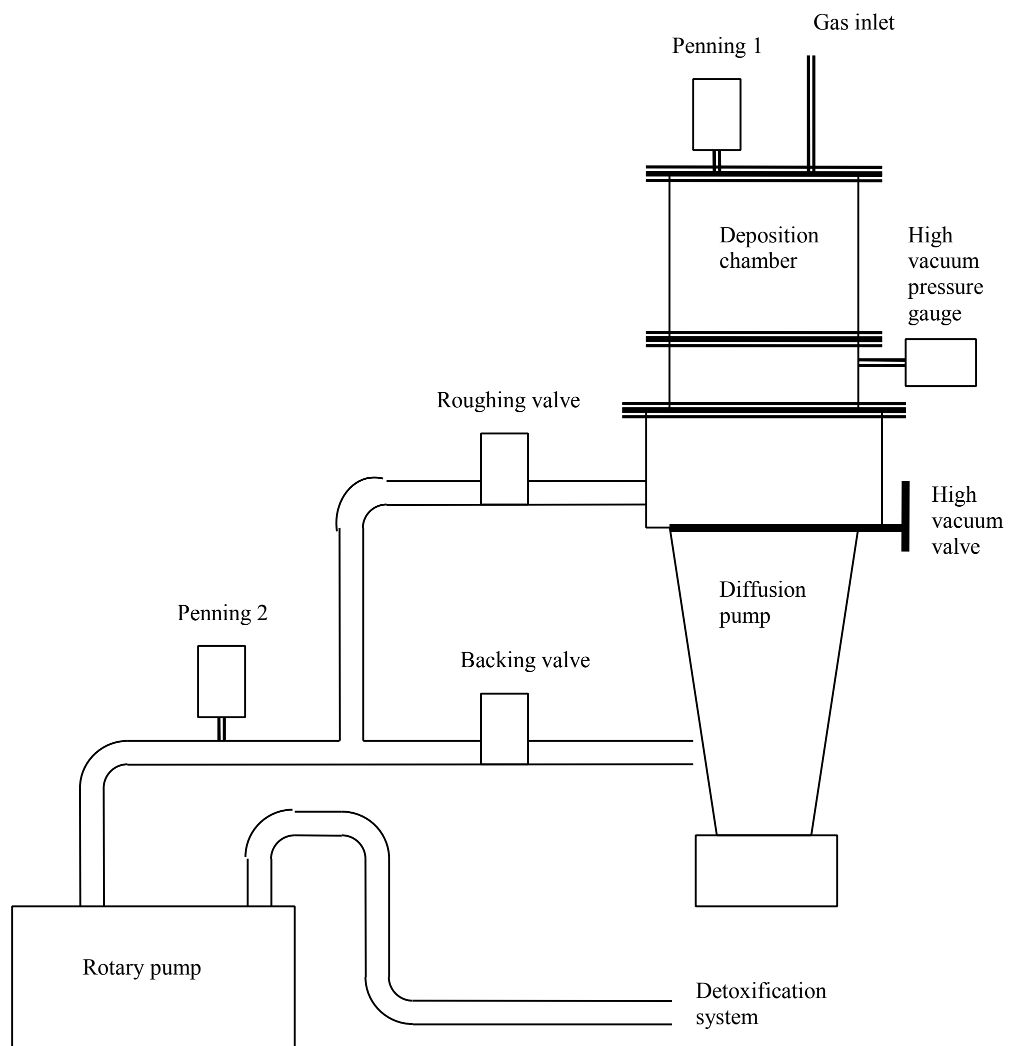

Figure 3.1: Overall view of the deposition system which mainly consisted of a deposition chamber, a diffusion pump, a rotary pump and a detoxification system.

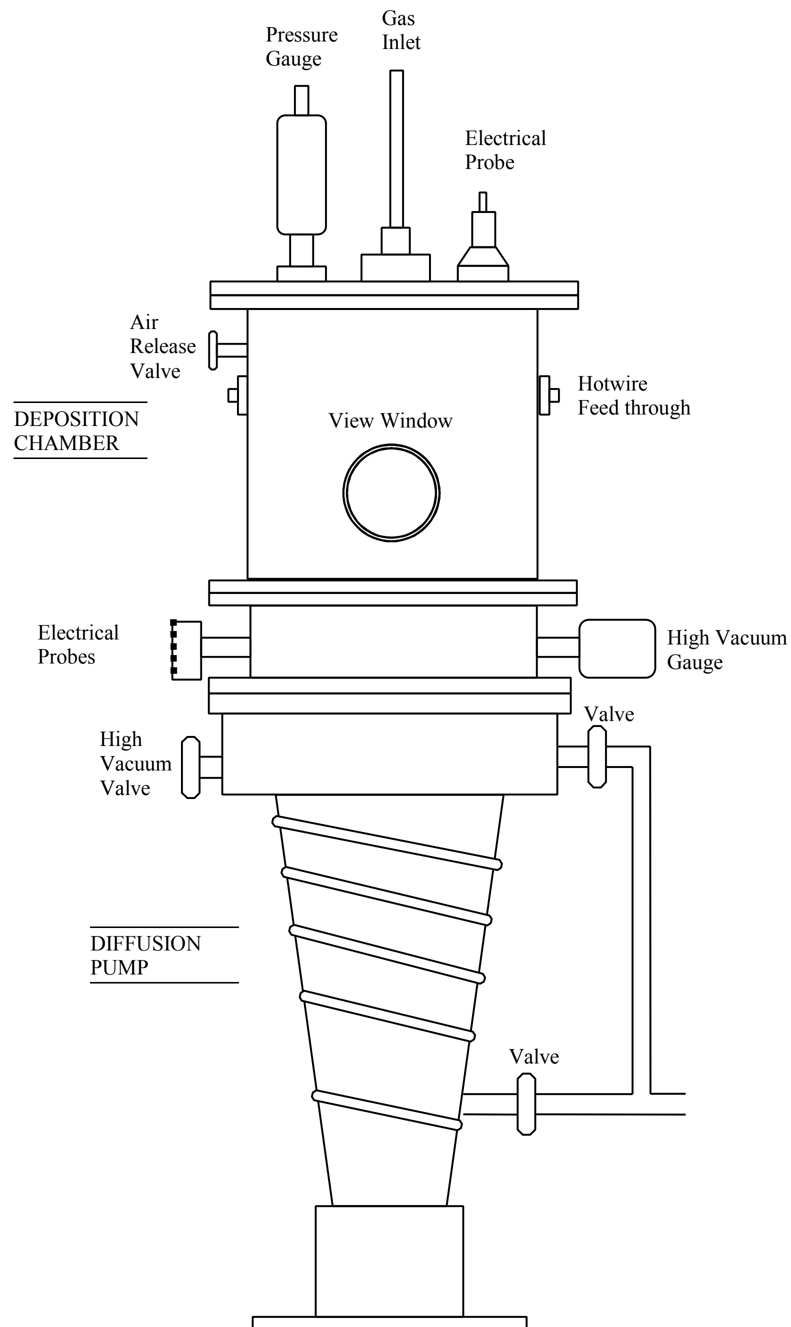

Figure 3.2: A schematic diagram of the deposition chamber and the diffusion pump.

3.2.1 The Deposition System

The deposition chamber was where the plasma reaction occurs in providing the thin films acquired for this research. Its power supply was made adjustable to suit for either radio frequency or direct current. For hot-wire deposition, the hot-wire filament was connected to DC power supply which generates voltage across the filament thus increases its temperature. Therefore the temperature of the filament was controlled by adjusting the applied DC voltage.

Figure 3.3 shows a schematic diagram of the deposition chamber. Gas inlets were designed to admit the required gas at fixed flow-rate via a mass flow controller. The gases involved in the preparation namely methane and silane were premixed before entering the deposition chamber and released vertically downwards through a shower. The substrate holder was placed 10.0 cm horizontally below the gas shower and could be heated to produce films at elevated deposition temperatures. For hot-wire deposition, the hot-wire filament which was made of 99.9% pure tungsten wire coiled into 6.0 cm length helix was placed at 4.0 cm above the substrate. The diameter of the coiled hot-wire filament was 3.0 mm.

Detailed diagram of the lower part of the deposition chamber is shown in Figure 3.4. This part places the substrate holder and connects the deposition chamber to the electrical and pumping systems. The substrate holder was designed to hold the substrates horizontally below the gas shower. Detailed dimension of the substrate holder are shown in aerial view and side view as in figure 3.5(a) and figure 3.5(b) respectively. It was made of stainless steel plates, 6.0 cm in diameter with built-in heater and thermocouple that were sandwiched between the plates. The substrate holder was also connected to electrodes for biasing purposes in direct current depositions. In order to insulate it from unnecessary electrical connections, glass legs were used in this set-up.

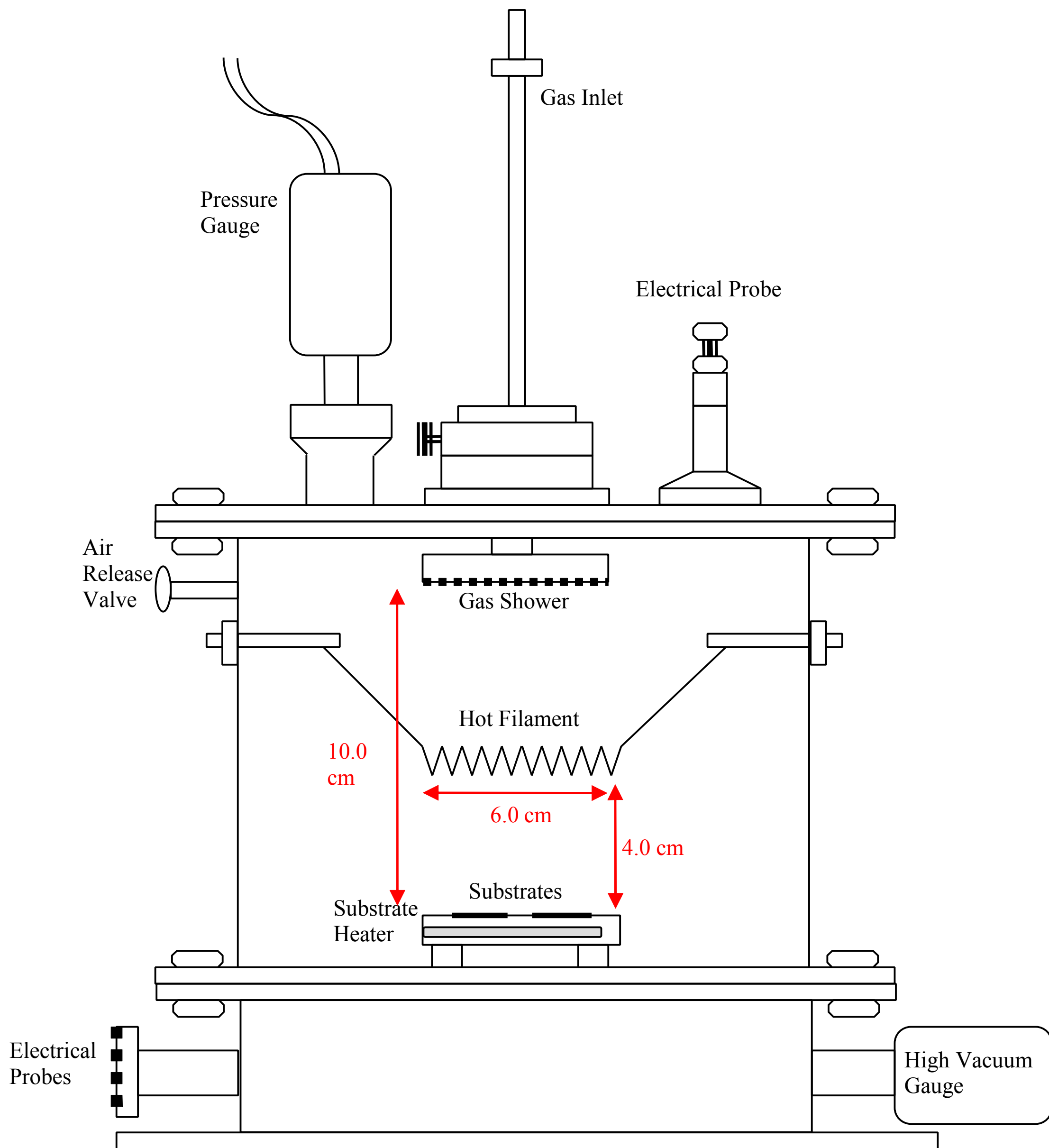

Figure 3.3: Schematic diagram of the deposition chamber.

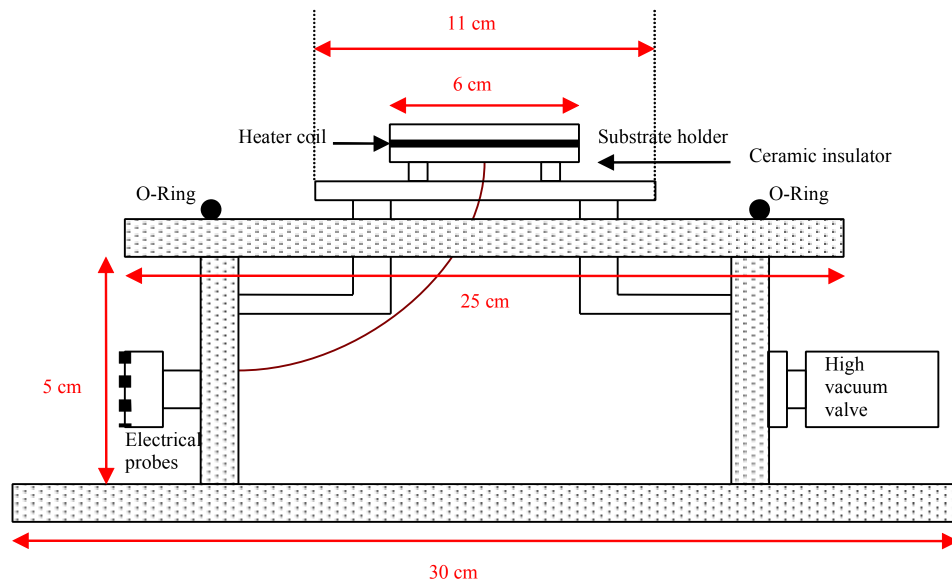

Figure 3.4: Detailed diagram of the lower part of the deposition chamber which connected to the electrical and pumping system.

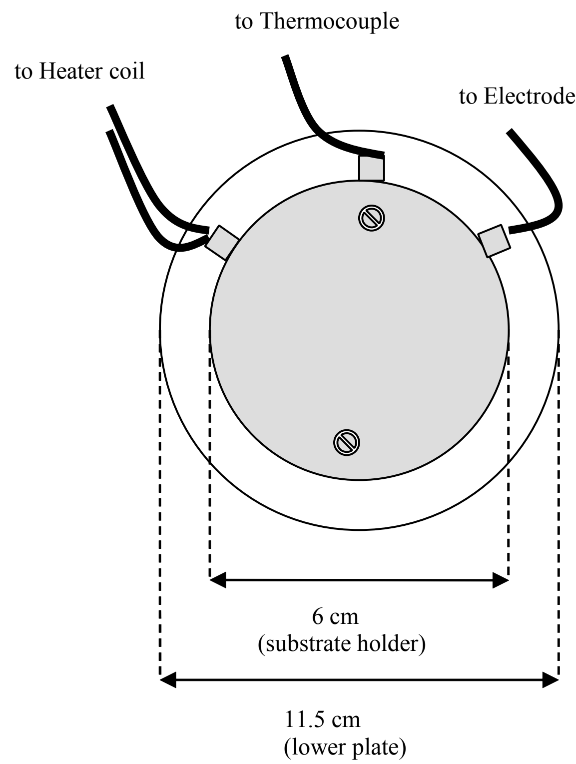

Figure 3.5(a): Aerial view of the substrate holder and its dimensions.

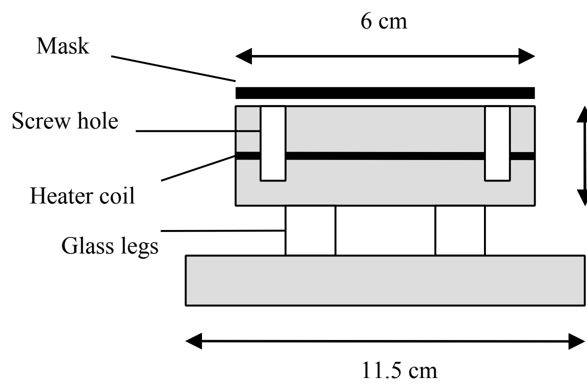

Figure 3.5(b): Side view of the substrate holder and its dimensions.

The pumping system for the plasma deposition system used in this research consisted of a diffusion pump and an EM28 Edwards Rotary Vacuum Pump and a Pirani-11 pressure meter. The pumping unit was fixed directly to the deposition chamber through an inlet catch-pot. The pressure in the chamber was measured by a Pirani-11 pressure meter which was connected via a PRE-10K gauge head that was fixed at the upper plate of the deposition chamber. The pressure meter has a range of 10^{-2} to 1.0 mbar. Throughout this work, the chamber pressure was maintained at a base pressure of about 10^{-6} mbar by a rotary and a diffusion pump to ensure the purity of the fabricated films. Excess gas was pumped out of the deposition chamber via one way valves that allow the gases to flow into the rotary pump. From the rotary pump, the gases were channeled to the detoxification tank for it to be safely diluted.

3.2.2 The Gas Distribution System

The gas distribution lines were made of 0.25-inch stainless steel tubing. It connected the deposition chamber to the various gas cylinders namely silane (SiH_4), methane (CH_4), and hydrogen (H_2) and nitrogen (N_2). The silane gas, being a heavily toxic gas was placed in a gas safety cabinet to ensure safety in case of leakage. Silane gas was first flown through a special gas regulator (Soxal 450-BS4-100) with special purging system. This purging system was connected to a nitrogen gas cylinder. The operating procedure for film deposition using silane gas is detailed in Appendix B.

Gases from the cylinders were separately directed through these tubing to a gas distribution panel that distributes the gases to various systems in the laboratory. Before reaching the deposition chamber, the gases had to go through separate metering valves, which then direct the gases to separate mass flow meter controllers. The mass flow meter controllers, which were connected to the system, monitor the gas flow rates. On

exiting the flow meters, the gases pass through one way valves to prevent back flows. For safety purposes, a bypass line is made after the metering valve of the silane line to allow silane gas to be pumped out even if a blockage occurs at the mass flow controller. Finally, the silane gas and other gases were joined at a single gas line, which directed the mixed gases into the deposition chamber.

3.2.3 The Detoxification System

In this experimental set-up, the detoxification system was directly attached to the exhaust of the rotary pump. The detoxification system, which was meant to dilute the toxic gases, removed excess silane. It consisted of a nitrogen gas line, which was bled into the oil bath of the rotary pump and a plastic container containing a solution of potassium permanganate ($KMnO_4$). The exhaust from the pump unit was directed to the $KMnO_4$ container. In this container, silane was transformed into harmless products as the following chemical reaction occurs.

$$2KMnO_4 + SiH_4 \rightarrow 2KMnO_2 + K_2SiO_4 + 2H_2$$

The excess silane gas was totally eliminated by the chemical process.

3.3 Preparation of SiC thin films

In this work, crystal silicon and sodalime glass substrates were used and cut to a size of 2.0 cm by 2.0 cm square. Two types of substrates were used in this work to accommodate to the needs of characterization equipments. All the substrates used were cleaned according to the cleaning procedures and placed on the substrate holder. Pre deposition and post deposition procedures had been observed strictly because it is very important to make sure that the system is free from any leakage since silane gas used in the deposition process is a highly toxic gas.

3.3.1 Substrate Cleaning Procedure

The most important requirement before starting any deposition was to clean the substrate from any dust, organic and inorganic matter that was trapped on the surface of the substrate which could significantly influence the properties of the film prepared. The substrate cleaning procedure underlined for glass substrate and crystal silicon substrate have to be followed very strictly. Once the substrate was considered clean, it was placed immediately in the reaction chamber to avoid recontamination. Different procedures were done for silicon substrate and glass substrate.

(a) Silicon Substrate

The crystal silicon wafer was first cut into small pieces and rinsed with deionized water. Then they were boiled for about 10 minutes in a solution of H_2O : H_2O_2 : HCl with a ratio of 86 : 11 : 3 respectively. Then the small pieces of silicon were rinsed with deionized water in order to wash out any inorganic excess on its surface. The silicon pieces were then immersed in a solution of H_2O : H_2O_2 : NH_4OH with a ratio of 7 : 3 : 3 respectively to remove any organic contamination. Then again they were rinsed in deionized water. After that the silicon pieces were immersed in a solution of H_2O : HF with a ratio of 10 : 1 respectively. Finally the silicon pieces were rinsed again in deionized water.

(b) Glass Substrate

Similar to the crystal silicon substrate, the sodalime glass substrate was first cut into small pieces. Then the small glass pieces were immersed in a beaker containing soap water. The whole beaker was then put into the ultrasonic bath for about 15 minutes. Then the glass substrates were rinsed in distilled water followed by acetone and ethanol. Finally they were rinsed again in distilled water.

3.3.2 Pre deposition Procedure

The pre deposition procedure started with pumping the deposition chamber using the rotary pump unit until the pressure was about 0.05 mbar. Then the gas lines were pumped stage by stage starting with opening the valves leading to the mass flow controller. Then the flowmeters were fully opened followed by the metering valves. Finally, the valves at the gas cylinders were opened.

The lines were pumped until the pressure of the entire system was less then 0.1 mbar. The next step was purging the silane gas line with oxygen-free nitrogen gas in order to remove any excess of silane from the previous deposition. After purging, the silane line was filled with nitrogen. Once the system was detected to be free from leakage, it was pumped down again before it was set into operation.

3.3.3 Post deposition procedure

Turning off the hot-wire power supply and DC power supply ended up the glow discharge process. The silane gas tank regulator was then closed and so was the methane gas. The gas line was pumped until the flowmeter indicated zero flow rate readings for all gases and the chamber pressure went down to 0.05 again. Finally, the silane gas line was purged again with nitrogen in order to flush out any excess silane in the line. The nitrogen gas line which lead to the oil bath of the rotary pump was closed after there was no more silane flowing in the line.

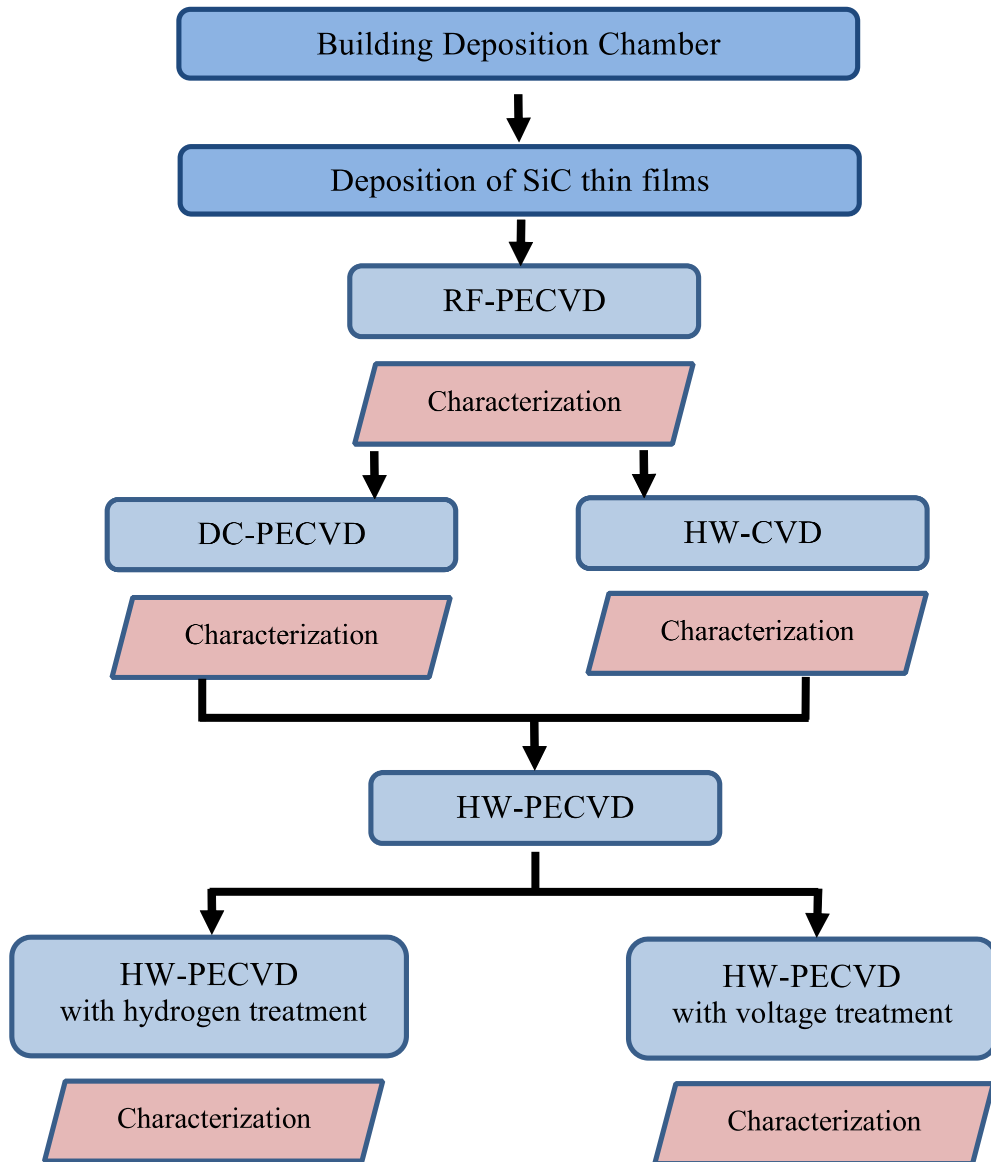

Figure 3.6: Flowchart of the work which led to the deposition of SiC thin films by the new hybrid HW-PECVD system.

Table 3.1: The parameters used for each deposition technique.

	RF-PECVD			DC-PECVD			HW-CVD			HW-PECVD			
Gas Flow Rate, F (sccm)	Silane SiH_4	Methane CH_4	Gas Flow Rate Ratio $R=F_{CH_4}/F_{SiH_4}$	Silane SiH_4	Methane CH_4	Gas Flow Rate Ratio $R=F_{CH_4}/F_{SiH_4}$	Silane SiH_4	Methane CH_4	Gas Flow Rate Ratio $R=F_{CH_4}/F_{SiH_4}$	Silane SiH_4	Methane CH_4	Hydrogen H_2	Gas Flow Rate Ratio $R=F_{CH_4}/F_{SiH_4}$
	10	15	1.5	5	10	2	5	10	2	5	10	nil	2
	5	12	2.4	5	20	4	5	20	4	5	70	nil	14
	5	20	4.0	5	30	6	5	30	6				
	5	45	9.0	5	50	10	5	50	10	5	70	30	1:14:6
	5	100	20	5	70	14	5	70	14	5	70	30	1:14:6
Deposition Pressure	8.0×10^{-1} mbar			5.4×10^{-1} mbar			5.2×10^{-2} mbar			5.2×10^{-2} mbar			
Substrate Temperature	250°C			350°C			350°C			350°C			
Filament Temperature	Non-applicable			Non-applicable			1700°C			1700°C			
Applied Voltage/Power	15 W, 13.56 MHz			1000 V			1000 V			1000 V			
										Voltage treatment: 1000 V, 1300 V, 1400 V, 1800 V			
Deposition Time	60 minutes			60 minutes			5 minutes			5 minutes			
										Hydrogen treatment: 1 min., 2 min., 3 min.			

3.4 Deposition Procedure of SiC thin films

In this work, deposition process was done at room temperature using different gas flow rates. The desired methane and silane flow rates were set on the mass flow controller. Then the cleaned glass and crystal silicon substrates were placed on the substrate holder. The system was then pumped down to a base pressure of about 0.05 mbar. The pre deposition procedure was carried on until it was save to operate using silane gas. Then nitrogen was introduced slowly into the oil bath of the rotary pump to dilute away contaminants and excess silane. All the parameters used in this work was selected after a series of try and error on the newly built system with the guide of other works done elsewhere. The performance of the deposition chamber was done based on the reliability of the chamber pressure on the silane, methane and hydrogen gas flow rate. The charts on Appendix B2 shows that the newly built chamber was working consistently due to change in gas flow rate and pressure.

3.4.1 Radio Frequency Plasma Enhanced Chemical Vapour Deposition

PECVD technique was employed to prepare a series of silicon carbide thin films in the presence of CH_4 and SiH_4 plasma. Pure SiH_4 (99.9995%) and pure CH_4 (99.99%) gases were allowed to flow at different flow rates so as to result in different methane to silane gas flow rate ratio between 1.5 and 20. The gas ratio was defined as $R = F_{CH4}/F_{SiH4}$ with F_{CH4} and F_{SiH4} being the flow rate of methane and silane gases respectively. For $R = 1.5$, silane gas was flown at 10 sccm and methane gas was flown at 15 sccm. For the rest of the sample, silane gas flow rate was fixed at 5 sccm and methane was flown at 12, 20, 45 and 100 sccm to result in R = 2.4, 4.0, 9.0 and 20 respectively. During the deposition process, the chamber pressure and the substrate temperature were maintained at 0.8 mbar and 250°C respectively. The gas ratio,

substrate temperature and chamber pressure used for RF-PECVD technique was slightly differed from values used in other techniques due to unstable deposition conditions such as fluctuation in the gas pressure which resulted in unexpected film quality. However, these values were kept in the same range for the purpose of comparison. The SiH_4 and CH_4 plasma was operated at 13.56 MHz and r.f. power of 15W during the deposition. Deposition time was fixed at 60 minutes for each preparation.

3.4.2 Direct Current Plasma Enhanced Chemical Vapour Deposition

For direct current deposition, silicon carbide thin films were prepared using a direct current, plasma enhanced chemical vapor deposition (DC-PECVD) system at different ratios of methane to silane gas flow rate. Silane gas flow rate was fixed at 5 sccm while methane gas flow rate was varied at 10, 20, 30, 50 and 70 sccm. Gas flow rate ratio was defined as $R = F_{CH4}/ F_{SiH4}$ resulting in a series of R = 2, 4, 6, 10 and 14. The chamber pressure during deposition was maintained at 5.4 x 10^{-1} mbar. The substrate temperature was kept at 350°C and the glow current maintained at 10 mA for all depositions.

3.4.3 Hot-Wire Chemical Vapour Deposition

In hot-wire chemical vapor deposition (HW-CVD) technique, hot-wire was the essential of the system. The hot-wire filament was made of tungsten wire of 0.5 mm diameter, coiled into a 4.0 cm helix. Substrates used in this work were made of glass and crystal silicon (c-Si), positioned horizontally at 4.0 cm below the tungsten wire. Silane gas was allowed to flow at 5 sccm for every deposition while methane gas was flown at five different flow rates of 10, 20, 30, 50 and 70 sccm. The gas flow rate ratio was defined as $R = F_{CH4}/ F_{SiH4}$ where F_{CH4} and F_{SiH4} are the gas flow rates of methane

and silane gas respectively. The chamber pressure during deposition was maintained at 5.2 x 10^{-2} mbar. The filament temperature was approximately 1700°C and the substrate was pre-heated to a temperature of 350°C for each deposition.

Deposition process took place according to the following procedure: With the silane valves closed, silane gas was first flown into the deposition chamber and the chamber pressure was measured. When the pressure had came to a stable state, methane gas was then allowed to flow into the chamber. Again, the new chamber pressure was measured. After the chamber pressure stables, the glow discharge was started by applying a required voltage across the hot-wire. As the deposition took place, parameters such as pressure, gas flow rate, ionization current and the hot-wire current were monitored every 5 minutes and maintained at the desired settings. At the end of the deposition, the hot-wire power supply was turned off thus stopping the discharge process.

3.4.4 Hot-Wire Plasma Enhanced Chemical Vapor Deposition

As the deposition of silicon carbide thin films through DC and hot-wire techniques studied in this work produces interesting results in a rather contrary manner, it is inevitable to further investigate the properties of films produced by a combination of the two techniques. Therefore in this research, an experimental set-up which consists of both techniques was established. In this technique, DC-PECVD and HW-CVD was combined in the effort to produce better quality silicon carbide thin films. Hot-wire filament was inserted in the deposition chamber as described earlier. The combined deposition technique was referred to as 'HW-PECVD technique'. The parameters of this experimental set-up follows the procedures of the hot-wire deposition technique with an addition of 1000 V direct current (DC) voltage that was applied across the deposition

chamber. This means that during deposition of the silicon carbide thin films, the plasma glow discharge would be contributed by both the hot-wire filament and the potential difference across the electrodes which is connected to the DC voltage. The glow current was maintained at 10 mA while the voltage was applied accordingly.

From the previous experiments, the highest optical energy gap was obtained from the deposition at the highest CH_4 to SiH_4 gas flow rate ratio, R=14. Therefore, in the next experiments where new parameters were introduced, only this ratio was being utilized. As the experiments proceed, hydrogen gas was also introduced into the plasma.

In the HW-PECVD deposition technique, hydrogen was utilized as a surface treatment factor with various treatment time of t = 1 minute, t = 2 minutes, and t = 3 minutes. For this experiment, only the highest gas flow rate ratio R=14 was used and hydrogen gas was allowed to flow at 30 sccm.

In order to study the effect of applied direct current voltage, the experiment was expanded by preparing silicon carbide thin films at different applied direct current voltage of 1000 V, 1300 V, 1400 V and 1800 V. The hot wire filament temperature was maintained at 1700°C and deposition time was fixed to 5 minutes due to technical constrictions.

3.4.5 Deposition with Hydrogen Plasma Surface Treatment

Taking into account the etching effects of hydrogen atoms, a set of silicon carbide thin film samples were prepared by this technique. For this set of deposition, a mixture of silane (SiH_4), methane (CH_4) and hydrogen (H_2) gases were allowed to flow into the chamber at a flow rate ratio of SiH_4:CH_4:H_2 = 5:70:30 sccm on the combination of hot-wire and direct current basis. Deposition was allowed for three minutes before the hot-wire filament was switched off and only hydrogen gas was allowed to flow for

the purpose of surface treatment. During the treatment process, direct current power was still turned on. Then the three minutes deposition process which was followed by surface treatment was repeated for a total of four cycles. The deposition with hydrogen treatment procedure was done in three procedures. Each procedure was differed by surface treatment time duration consisting of one minute, two minutes and three minutes.

3.5 Analytical Techniques

Films deposited on glass substrates were scanned using Jasco UV-Vis-NIR 3102-PC double beam spectrophotometer in the range of 200 to 2500 nm for optical observation purposes. Optical energy gap of the films were deduced from the Tauc's plot. The film structure and chemical bonding configurations were investigated by using Fourier-Transform Infrared (FTIR) and micro-Raman spectroscopy. FTIR spectroscopy were done on films deposited on c-Si substrates within the scanning range of 400 to 4000 cm^{-1} using Perkin-Elmer 2000 FTIR spectrometer. Raman spectroscopy was carried out on silicon carbide thin films prepared on c-Si to provide information on the structural properties of the films. Renishaw System 2000 Raman Spectrometer was utilized for this purpose.

3.5.1 Ultraviolet/Visible/Near Infrared (UV/Vis/Nir) Spectroscopy

The ultra violet-visible spectrum (UV-VIS) was used to characterize the optical properties of the films prepared. Parameters obtained from this technique were the refractive index (n), the film thickness (d), and the optical energy gap (E_g). The optical transmission spectrum was obtained using the Jasco UV-VIS-NIR 3102-PC double beam spectrophotometer in the range of 200 to 2500 nm. The instrument consisted of a

light source, a monocromator, a sample compartment which holds a reference and a sample, a photo detector and a computer to control the measurement.

In starting the measuring process, the spectral baseline was first obtained. In order to obtain the spectral baseline, two slides of glass were placed one in each reference and sample holder. Once the spectral baseline was obtained, the glass in the sample holder was removed and replaced by the sample deposited on glass. Then the measurement begun and the optical transmission spectrum was observed.

The optical band gap was determined from the Tauc formula as follows,

$$(\alpha h\nu)^{1/2} = B(h\nu - E_{opt.}) \qquad \text{------(3.0)}$$

Here, α was the absorption coefficient and $h\nu$ was the photon energy. It was actually obtained by plotting $(\alpha h\nu)^{1/2}$ versus $h\nu$ curve. The optical band gap was the value of meeting point by extrapolating the linear region was the curve to $h\nu$ axis in the high absorption region. The parameter B depended on the product of the oscillator strength of the transition, the deformation potential and the mean deviation of the atomic coordinates. It could be taken as a measurement of the structural disorder in a-Si_{1-x} C_x: H thin films. The higher the B value, the lower the degree of structural disorder (Zhang *et al.,* 2008, Conde *et al.,* 1999).

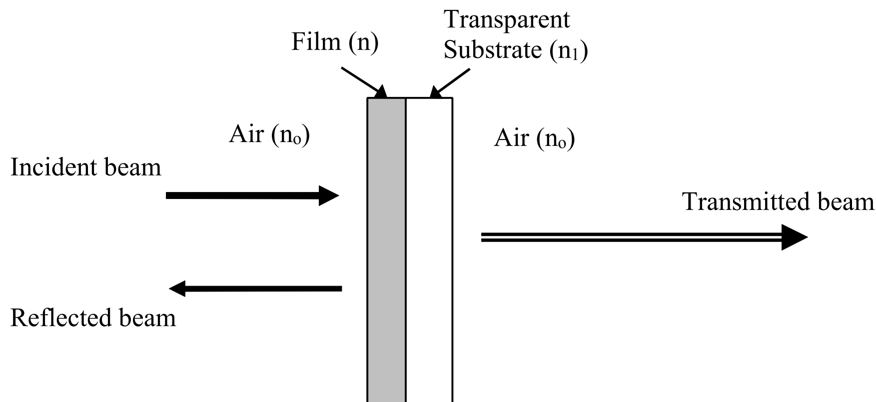

Figure 3.7: A thin film on a transparent substrate.

The refractive index and the thickness of the film were deduced from the optical transmission spectrum of the film using the interference fringes in the low absorption region. In calculating the values, combination of Manifacier technique and Davies technique was used. The configuration of film on a transparent substrate is shown in Figure 3.7. The values of the refractive index, n, and the thickness, d, of the film were deduced from the interference pattern in the long wavelength region. The transmission can be expressed as

$$T = \frac{AX}{(1-B)(1-CX^2)} \qquad \text{------(3.1)}$$

where $A = (1 - R_1)(1 - R_2)(1 - R_3)$

$B = R_2 R_3$

$C = R_1 R_2 + R_1 R_3 (1- R_2)^2$

$$X = exp\,(-\alpha d) \qquad \text{------(3.2)}$$

And R_1 = reflectance at air-film

R_2 = reflectance at film-substance

R_3 = reflectance at substance-air

α = absorption coefficient

d = film thickness

Using the Manifacier technique which is accurate when transmission is almost 100%, the refractive index of film is

$$n = \sqrt{N + (N_2 - n_o^2 n_1^2)^{1/2}} \qquad \text{------(3.3)}$$

where $N = \frac{(n_o^2 + n_1^2)}{2} + 2n_o n_1 \frac{(T_{\max} - T_{\min})}{T_{\max} T_{\min}}$ ------(3.4)

The film thickness, d, can be calculated from the following equation.

$$d = \frac{M(\lambda_1 \lambda_2)}{2[\lambda_1 n_2(\lambda_2) - \lambda_2 n_1(\lambda_1)]} \qquad \text{------(3.5)}$$

where M was the number of complete oscillations between two extremes, and $n_2(\lambda_2)$ and $n_1(\lambda_1)$ were refractive indices at λ_2 and λ_1 where the two extremes were observed. In manipulating Manifacier technique, greater accuracy was gained if n was determined at the longest wavelength.

In the Davies technique, equation 2nd sin θ = mλ was used. Since in the system, θ is 90°, the equation becomes 2nd = mλ where m = 1/2, 1, 3/2, …. From the transmission spectrum, wavelengths where maximum and minimum occurred were determined from the longest wavelength downwards. Then the values of mλ/2 was plotted versus wavelength and the value of m was changed until a curve similar to Figure 3.8 was obtained. The particular value of m was assumed to be the correct m value for the spectrum.

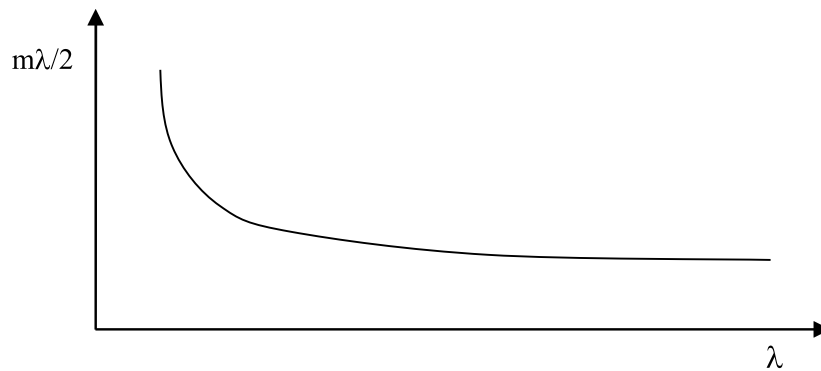

Figure 3.8: The curve for the correct m value.

The n value at the longest wavelength corresponds to the correct m was then used to determine the film thickness, d where $d = \frac{m\lambda}{n}$. Then, this d was used to determine the values of n for the rest of the wavelengths.

Plotting these values of n versus $\frac{1}{\lambda^2}$ will result in a linear relation *(y = c + mx)* and fitting it to the following Cauchy equation

$$n = a + \frac{b}{\lambda^2} \qquad \text{------(3.6)}$$

will allow us to determine the values of a and b. a would be the intercept at the vertical n-axis and was called the static refractive index of the film or also known as n_o. b would be taken as the slope of the line produced. If n for the whole spectrum was determined, dispersion of the refractive index could be obtained.

From equation 3.2, absorption coefficient, α, can be written as

$$\alpha = \frac{1}{d}\ln\left(\frac{1}{X}\right) \qquad \text{------(3.7)}$$

where $X = -A + 2CT(1-B)\sqrt{A^2 + 4CT^2(1-B)^2}$ ------(3.8)

In determining the optical energy gap, photon energy for the whole spectrum was calculated through equation 3.8. α was then calculated for the whole spectrum. Then the values of $\sqrt{\alpha E}$ was plotted versus E. From its linear portion, energy gap, E_g could be determined by dividing c over m where c was its intercept and m was its slope, $E_g = \frac{c}{m}$.

3.5.2 Fourier Transform Infrared (FTIR) Spectroscopy

Infrared spectroscopy was used to determine the content of chemical bonds including hydrogen and carbon bonds based on the integrated absorption intensity of stretching mode bonds such as $Si\text{-}H_n$ (n=1,2) at 2000-2200 cm^{-1}, $C\text{-}H_2$ at 2890 cm^{-1}, $C\text{-}H_3$ at 2960 cm^{-1} and Si-C at 790 cm^{-1} (Kaneko *et al.,* 2005).

From the FTIR spectra, the integrated absorption intensity of the stretching mode of $Si\text{-}H_n$ and $C\text{-}H_n$ bonds were calculated and the content of bonded hydrogen was quantitatively deduced using the absorption cross-section. Using a similar process and spectra pattern separation, the content of Si-C bonds was also deduced and the hydrogen content ratio of the films was obtained.

The crystal silicon substrate without any deposition was first scanned as background. After the background spectrum was obtained, the empty substrate was replaced by the sample deposited on a crystal silicon substrate. The FTIR spectrum for the film is the resultant of the sample spectrum minus the background spectrum. The spectrum was averaged over 20 scans.

In this work, the Si-H environment was characterized by a bond-stretching mode at 2000 cm^{-1} and a bending-mode at 630 cm^{-1}. The transmission spectra was first converted to absorption coefficient spectra using equation 3.9. Then the Gaussian or Doppler lineshape is used to deconvolute component peaks from the absorption spectrum. The equation used for the Gaussian lineshape was given in equation 3.10.

$$\alpha(\omega) = \frac{1}{d}\ln\frac{100}{T\%} \qquad \text{------(3.9)}$$

$$\alpha(\omega) = \alpha(\max)\exp - \left[\frac{4(\ln 2)(\omega - \omega_o)^2}{\Delta\omega}\right] \qquad \text{------(3.10)}$$

where

$$\alpha(\max) = \frac{2S_{band}\sqrt{\ln 2}}{\Delta\omega\sqrt{\pi}}$$

and $S_{band} = \alpha(\omega)\, d\omega$ ------(3.11)

S_{band} was the area under the curve, $\Delta\,\omega$ was the full width half maximum of the absorption peak, $\alpha(max)$ was the maximum absorption coefficient and ω_o was the peak position.

In the form of

$$y = A\ exp\ (-Bx) \qquad \text{------(3.12)}$$

Equation 3.12 can be rewritten with

$$A = \frac{S_{band}\sqrt{B}}{\sqrt{\pi}}$$

$$B = \frac{4\ln 2}{(\Delta\omega)^2}$$

and $\quad x = (\omega - \omega_o)^2$

Rewritting equation 3.12,

$$ln\ y = ln\ A - B(\omega - \omega_o)^2. \qquad \text{------(3.13)}$$

The integrated intensity of the absorption peak which represents a bonding configuration was therefore

$$I = \frac{\alpha(\omega)}{\omega_0}d\omega \qquad \text{------(3.14)}$$

The integrated intensity can also be derived from equation 3.13 thus be written as

$$I = \frac{S_{band}}{\omega_o} \qquad \text{------(3.15)}$$

Calculating the hydrogen content was the continuation from integrated intensity. Assuming the hydrogen concentration in the film as N, thus N = AI with A= 1.6 x 10^{19} cm^{-1} for the Si-H wagging mode at 640 cm^{-1}. The microstructure parameter, R was then determined by the following equation.

$$R = \frac{I_{2100}}{I_{2100} + I_{2000}} \qquad \text{------(3.16)}$$

The total hydrogen content is

$$H\% = \frac{N}{N_{Si}} \qquad \text{------(3.17)}$$

with N_{si} = 5 x 10^{22} is the silicon atom concentration in crystal silicon samples. The microstructure parameter was utilized to determine the hydrogen content at the internal surface of microvoids and at isolated Si-H bonds.

Hydrogen content at the internal surface of the microvoids was

$$H(v) = R \times H\% \qquad \text{-------(3.18)}$$

Hydrogen content at isolated SiH bonds was

$$H(SiH) = (1 - R)\, H\% \qquad \text{-------(3.19)}$$

The values of *H(v)* and *H(Si-H)* indicates the structure of the film. If the value of *H(SiH)* is bigger than *H(v),* the film has an amorphous structure whereas if *H(v)* dominates the film with its value bigger than *H(Si-H),* the film has a columnar structure.

3.5.3 Micro-Raman Scattering Spectroscopy

Micro-Raman Spectroscopy was done in order to investigate the molecular vibration frequency which corresponds to the frequency changes caused by the scattering by molecules. Raman scattering was a useful, sensitive, precise, and non-destructive technique for the characterization and study of semiconductor materials. Raman characterization can give an indication of the degree of the crystalline structure of the CVD-grown films.

When light encounters the surface of a semiconductor, most of it is reflected, transmitted and absorbed due to first order elastic interactions with electrons, phonons

and impurities. These processes do not involve any change in the phonon frequency. However, a small part of the radiation interacts in-elastically with phonon modes thus producing photons whose frequency were shifted from the incoming values. These photons were referred to as Raman-scattered photons. These photons can either gain energy by absorbing a phonon (anti-stokes shift) or lose energy by emitting a phonon (Stokes shift) according to the energy and momentum conservation rules;

$$\omega_s = \omega_i \pm \Omega$$

and

$$q_s = q_i \pm K$$

where ω_s and ω_i were the scattered and incoming photon frequencies respectively, q_s and q_i were scattered and incoming photon wave vectors respectively, Ω and K were the phonon frequency and wave vector respectively.

Since Raman scattering was inherently a weak process, a high power light source such as laser was usually used to obtain a measurable scattered intensity. In this work, micro-Raman spectroscopy was carried out on silicon carbide thin films prepared on c-Si substrates to provide information on the structural properties of the films. Renishaw System 2000 Raman Spectrometer was utilized for this purpose and the parameters used are shown in Table 3.2. Among the identifications that are of interest in this study are the silicon carbide TO and LO phonon vibration modes at around 796 and 965 cm^{-1} respectively, a broad shoulder at around 760 cm^{-1} which could be assigned to the amorphous phase of silicon carbide and a broad peak centered at about 490 cm^{-1} which was due to acoustic phonon modes of nanocrystalline silicon carbide. A broad bump at around 480 cm^{-1} was also identified as Si clusterization in amorphous phase. A sharp peak at 520 cm^{-1} would indicate the formation of microcrystalline-Si or LO mode of (100) Si substrate. Besides, a shifted spectrum to longer wavenumber would suggest

some contribution of microcrystalline component. Therefore, through analysis from the micro-Raman spectra, the structural nature of the silicon carbide films prepared in this work could be identified.

Table 3.2: The parameters of Renishaw System 2000 Raman Spectrometer utilized in this work.

Source	Ar^+ laser, 514.5nm
Laser power supply	25 mW
Spectral resolution	1 cm^{-1}
Spectral range	700-1900 cm^{-1}
Spatial resolution	1 mm
Laser spot size	1 mm
Capability	Spectrum

3.5.4 X-Ray Diffractometry

X-ray diffractometry (XRD) was the most widely used technique in materials characterization. It was based on the diffraction of X-ray radiation within the film structure. The X-ray radiation used for XRD measurement was in the spectral range of 5 – 20 keV. The typical penetration depth of X-ray in the sample was in the order of 100 µm. In the studies of polycrystalline specimens, X-ray beam of a single wavelength was used.

Diffractometry enables us to identify the crystal structure and quality by analyzing then comparing the spectrum with a database containing over 60 000 diffraction spectra of known crystalline substances, some of which were presented in Appendix B3. The basic function of a diffractometer is to detect X-ray diffraction from materials and to record the diffraction intensity as a function of the diffraction angle (2θ). Figure 3.9 demonstrates the geometrical arrangement of an X-ray diffractometer

which mainly consists of X-ray source, specimen and detector (Leng, 2008). The X-ray radiation generated by an X-ray tube passes through special slits which collimate the X-ray beam. The slits were made of a set of closely spaced thin metal plates parallel to the figure plane to prevent beam divergence in the direction perpendicular to the figure plane. A divergent X-ray beam that passes through the slits will then strikes the specimen. X-rays were then diffracted by the specimen and form a convergent beam at receiving slits before they enter a detector. By continuously changing the incident angle of the X-ray beam, a spectrum of diffraction intensity versus the angle between incident and diffraction beam was recorded.

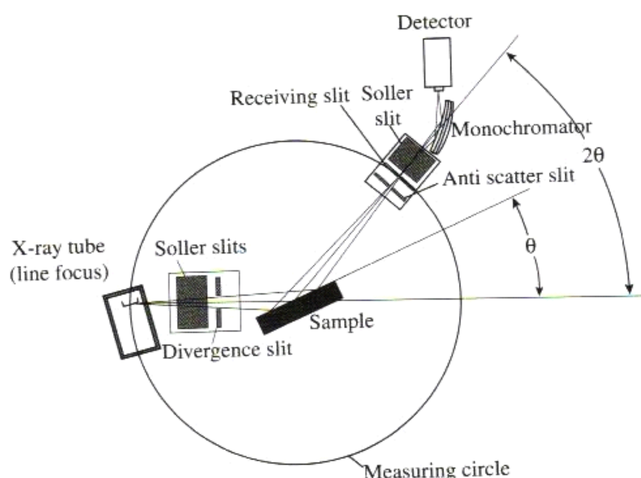

Figure 3.9: Geometric arrangement of X-ray diffractometer (Leng *et al.,* 2008).

Table 3.3: Parameters used for SIEMENS X-ray Diffractometer D5000 machine.

Scanning range 2θ	20 – 100°
Alpha angle (α)	2°
Step size	0.1°
Step time	5 s

In this work, SIEMENS X-ray Diffractometer D5000 machine was used with its parameters set according to Table 3.3. Data analysis done by the computer included peak angle, intensity, lattice constant and FWHM. Debye Scherrer Equation which relates the breadth of a specific phase to the mean crystallite size has been adopted in this work in order to determine crystallite size. Quantitatively, sharper peaks indicate larger crystallite size.

The equation takes the following form.

$$\beta = \frac{K\lambda}{L\cos\theta}$$

β was the width of the peak at half maximum intensity of a specific phase in radians, K was a constant that varied with the method of taking the breadth. In this work, K was taken as equivalent to 0.9. λ, which was the wavelength of the incident X-ray which was taken as 1.5406 Å, θ was the center angle of the peak and L was the crystallite length.

3.5.5 AFM Microscopy

The atomic force microscope (AFM) uses a very sharp tip to probe and map sample topography. The AFM detects near-field forces between the tip and sample, instead of detecting the tunneling current. Knowledge of the near-field forces acting between tip and sample is necessary in understanding the AFM working principles. The key element of the AFM is its microscopic force sensor. The most common force sensor is a cantilever. The tip is mounted at the end of a cantilever. The force detection is a based on a beam deflection method. The force between the tip and sample generates elastic bending of the cantilever. The amount of bending is monitored and recorded by position-sensitive photodiodes which are arranged in four quadrants. The photodiodes receive the laser beam reflected from the rear side of the cantilever, which often has a

thin metal coating, making it a mirror. Any small deflection of the cantilever will tilt the laser beam and change its striking position on the photodiodes. The difference between the two photodiodes signals indicates the amount of cantilever deflection. The amount of deflection then can be mathematically converted into the force on the tip, according to the elastic properties of the cantilever (Leng, 2008). Figure 3.10 shows a geometric set-up of the AFM machine.

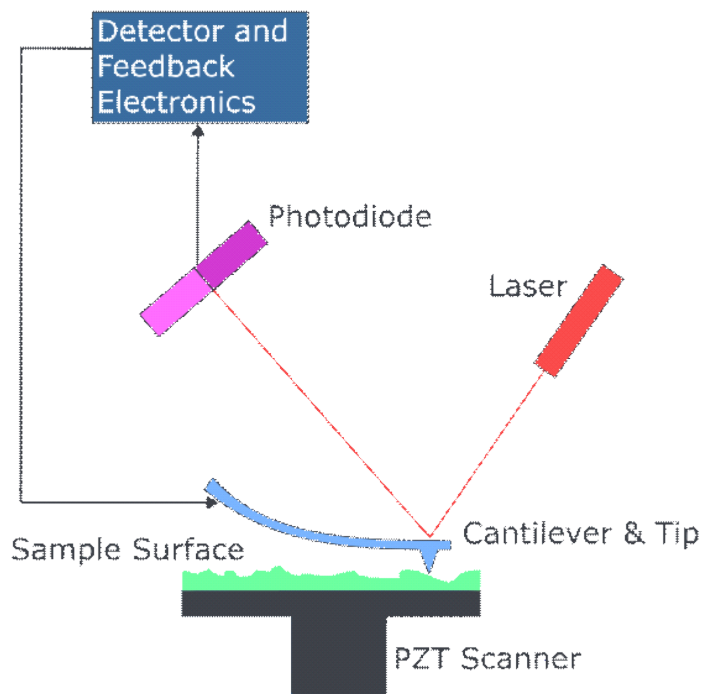

Figure 3.10: Geometric arrangement of an AFM machine.